ISSN 0030-400X, Optics and Spectroscopy, 2016, Vol. 120, No. 1, pp. 143–152. © Pleiades Publishing, Ltd., 2016.
Original Russian Text © V.A. Loiko, V.Ya. Zyryanov, A.V. Konkolovich, A.A. Miskevich, 2016, published in Optika i Spektroskopiya, 2016, Vol. 120, No. 1, pp. 158–168.

PHYSICAL OPTICS

Light Transmission of Polymer-Dispersed Liquid Crystal Layer Composed of Droplets with Inhomogeneous Surface Anchoring

V. A. Loiko[a], V. Ya. Zyryanov[b], A. V. Konkolovich[a], and A. A. Miskevich[a]

[a] *Stepanov Institute of Physics, National Academy of Sciences of Belarus, Minsk, 220072 Belarus*
[b] *Kirensky Institute of Physics, Siberian Branch, Russian Academy of Sciences, Krasnoyarsk, 660036 Russia*
e-mail: loiko@dragon.bas-net.by

Received October 14, 2014; in final form, July 8, 2015

Abstract—We have developed a model and realized an algorithm for the calculation of the coefficient of coherent (direct) transmission of light through a layer of liquid crystal (LC) droplets in a polymer matrix. The model is based on the Hulst anomalous diffraction approximation for describing the scattering by an individual particle and the Foldy–Twersky approximation for a coherent field. It allows one to investigate polymer dispersed LC (PDLC) materials with homogeneous and inhomogeneous interphase surface anchoring on the droplet surface. In order to calculate the configuration of the field of the local director in the droplet, the relaxation method of solving the problem of minimization of the free energy volume density has been used. We have verified the model by comparison with experiment under the inverse regime of the ionic modification of the LC–polymer interphase boundary. The model makes it possible to solve problems of optimization of the optical response of PDLC films in relation to their thickness and optical characteristics of the polymer matrix, sizes, polydispersity, concentration, and anisometry parameters of droplets. Based on this model, we have proposed a technique for estimating the size of LC droplets from the data on the dependence of the transmission coefficient on the applied voltage.

DOI: 10.1134/S0030400X16010112

INTRODUCTION

Controllable light scattering in composite liquid crystal (LC) materials exposed to the action of an external electric or magnetic field is one of the widely investigated and promising methods of the response formation in devices of information display, telecommunication, optoelectronics, and photonics [1–6].

Among composite LC materials, polymer-dispersed LC (PDLC) materials occupy a special place [4, 7, 8]. They are polymer films with LC droplets dispersed into them. In the regime of light scattering mode, electrooptical effects in PDLC films are realized by changing the configuration of LC molecules in droplets under the action of an external controlling field.

Two approaches that are used to control the electrooptical properties of PDLC films can be singled out.

One of them (which is traditional) is based on the classical Fréedericksz effect [7–10]. Its essence is as follows. The volume of LC droplets is exposed to the action of an external controlling field, which changes the orientation of LC molecules in the volume of LC droplets. In this case, the surface anchoring of LC molecules with the polymer matrix remains unchanged. After the switching off of the field, the internal orientational structure of LC droplets returns to the initial state because of the action of elastic forces that are inherent in LCs. The classical Fréedericksz effect underlies the operation of modern electrooptical LC devices.

Another approach is developed based on the so-called "local Fréedericksz transitions" [11, 12], which are related to transformations of the volume orientation of the optical axis (director) due to changes in the balance of the orienting action of different surface forces. A typical example is the reorientation of the layer of a nematic LC that is screened by a thin amorphous film (with a thickness of ~10 nm) from the crystalline substrate. In this case, the orienting actions of the film and substrate should be different, e.g., planar and homeotropic. A variation in the temperature of the film [13] or in its thickness [14] changes the balance between the orienting actions and initiates a reorientation of the LC layer. In practical applications, methods of modification of the boundary conditions involving the application of the electric field are in most demand. For example, the authors of [15] used for this purpose substrates coated by a ferroelectric LC polymer. An azimuthal reorientation of the director in an LC polymer upon a change in the polarity of the applied voltage causes the corresponding orientational transformation in the volume of the nematic that borders on this substrate.

The use of local Fréedericksz transitions creates the possibility for the development of new types of information display facilities. Therefore, the problem of searching for ways for their realization is important. One of these ways is the use of PDLCs on the surface of droplets of which inhomogeneous surface anchoring is created [16, 17]. In this case, the external action initially changes the orientation of LC molecules in a near-boundary layer of LC droplets, which then causes the reorientation of the entire LC volume. This approach is based on the mechanism of reorientation of the internal structure of LC droplets that is fundamentally different compared to the classical Fréedericksz effect and makes it possible to create PDLC layers with a low energy consumption.

Modification of the interphase surface anchoring is achieved by using ion-forming surfactants (surface-active agents) in the process of fabrication of PDLC films. Depending on the concentration of the surfactant, the direct or inverse regimes of the electrically controllable ionic modification of the interphase boundary can take place. The direct regime is realized at low concentrations of the surfactant. In this case, in the initial state, in the absence of a controlling field, nematic droplets have homogeneous tangential anchoring and bipolar configuration of local optical axes. The inverse regime [17] is realized at high concentrations of the ionic surfactant. In this case, the initial structure of nematic droplets has a radial configuration of the director with homogeneous normal boundary conditions. The action of the controlling electric field leads to the formation of regions with different types of the surface anchoring on the droplet surface. These regions determine the orientational structure of LC molecules in the droplet. The fractions of the regions with the normal and planar orientations and, correspondingly, the orientational structure of LC molecules depend on the magnitude of the field. In a strong field, homogeneous surface anchoring is realized. This kind of anchoring is opposite to the initial one, which is realized in the absence of a field; whereas planar anchoring is realized in the absence of a field, homeotropic anchoring takes place in a strong field and vice versa. It should be noted that LC droplets with modified surface anchoring are nothing else but Janus particles [18, 19] with controllable properties. One part of the droplet has planar anchoring, whereas the other part has homeotropic anchoring. Their ratio depends on the magnitude of the applied field.

In studies of light scattering by PDLC layers, it is necessary to take into account the optical anisotropy of the LC, changes in the surface anchoring and internal structure of droplets at the applied field, concentration of droplets, multiple scattering of light, and other parameters [4, 8]. Rigorous methods have not been developed for solving direct and inverse problems of light scattering by PDLC films that take into account the complex influence of the factors listed above. The main attention is paid to the development of approximate methods of solution, which make it possible to reveal basic features of the formation of the electrooptical response with the goal of its optimization [20–35].

In this work, based on the Foldy–Twersky approximation [36] to describe the mean field [8] and the anomalous diffraction approximation to describe the scattering by an individual particle [25, 37], we develop an optical model for the analysis of the coefficients of coherent (direct) transmission of light by a PDLC layer upon its illumination with linearly polarized and unpolarized monochromatic radiation. The model makes it possible to investigate layers with homogeneous [4, 8] and inhomogeneous [16, 17, 33, 35] interphase surface anchoring. A layer of polydisperse oriented ellipsoidal droplets of a nematic LC is considered. A relaxation method to solve the problem of minimization of the free energy volume density for finding the internal structure of LC droplets in relation to the ratio of the fractions of the surface that have normal and homeotropic anchoring is considered. The coherent transmission coefficient of a PDLC layer that consists of spherical LC droplets is analyzed taking into account the inhomogeneity of surface anchoring. The developed optical model is verified by comparison with experiment in the inverse regime of the ionic modification of the LC–polymer interphase boundary, in which radial structure of the director field is implemented in the absence of the applied field. The developed optical model makes it possible to solve problems of optimization of the electrooptical response of a PDLC layer with the goal to increase the contrast and the modulation depth of the forward-transmitted light depending on the parameters of the film and droplets in which homogeneous or inhomogeneous surface binding is realized, in particular, the sizes, the anisometry parameters, the polydispersity, the concentration of LC droplets, and the film thickness.

BASIC RELATIONS FOR COHERENT TRANSMISSION COEFFICIENTS OF A PDLC LAYER

Let us find the coherent transmission coefficients of a PDLC layer with thickness l upon its illumination by linearly polarized and unpolarized monochromatic radiation. Let the layer consists of LC droplets of ellipsoidal shape that are oriented in one and the same direction in the plane of the layer. We will choose a laboratory coordinate system (x, y, z) such that the x axis will coincide with the normal to the PDLC layer, while the (y, z) plane coincides with its frontal boundary (Fig. 1). Let the long axes of LC droplets in the layer be oriented along the y axis of the (x, y, z) lab-

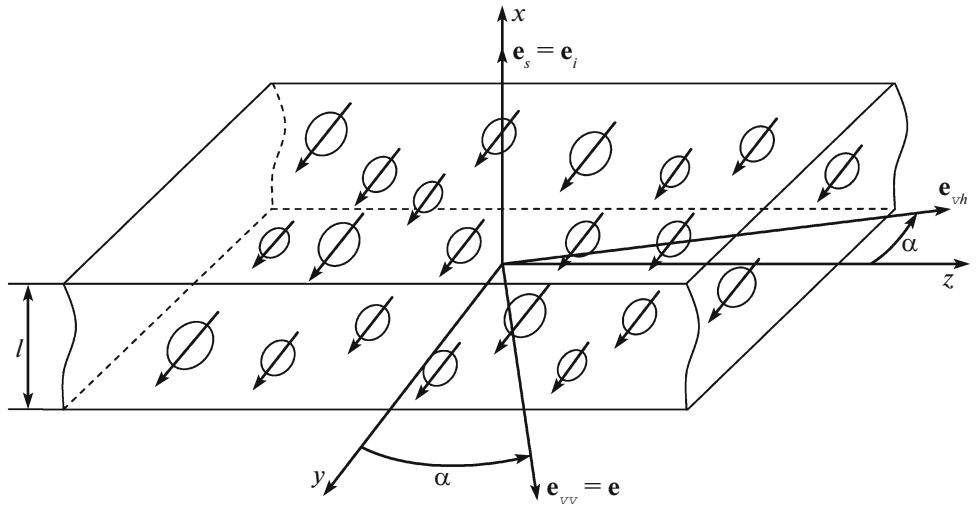

Fig. 1. Schematic representation of the illumination geometry and orientational structure of a PDLC layer. Here, (x, y, z) is the laboratory coordinate system; l is the layer thickness; $\mathbf{e}_i$ is the unit vector in the direction of incidence of the light; $\mathbf{e}_s$ is the unit vector of the forward-scattered wave; $\mathbf{e}_{vv}$ and $\mathbf{e}_{vh}$ are the unit vectors of the vv- and vh-components of the scattered wave with their polarizations in the plane of polarization of the incident wave $(\mathbf{e}_i, \mathbf{e})$ and in the plane that is orthogonal to it $(\mathbf{e}_i, \mathbf{e}_{vh})$, respectively; and α is the polarization angle of the incident light.

oratory coordinate system. Optical axes **N** (directors) [4] of droplets coincide with their long axes and, correspondingly, are also oriented along the y axis. The internal structure and anisometry are the same for all droplets.

Initially, let us consider the case of illumination along the normal by a linearly polarized plane wave. In Fig. 1, **e** is the unit polarization vector of the incident wave; α is the polarization angle of the incident light, which is counted from the y axis; and $\mathbf{e}_s$ is the unit vector of the scattered wave. In terms of the model to be developed, we consider the case of scattering in the direction of the wave vector of the incident wave; i.e., $\mathbf{e}_s = \mathbf{e}_i$. The unit vectors $\mathbf{e}_{vv}$ and $\mathbf{e}_{vh}$ define the vv- and vh-components of the coherent (forward-transmitted) wave: the vv-component is polarized in the plane of polarization of the incident wave $(\mathbf{e}_i, \mathbf{e})$, while the vh-component is polarized in the plane that is orthogonal to the plane of polarization of the incident wave $(\mathbf{e}_i, \mathbf{e}_{vh})$. In the experiment, the vv- and vh-components correspond to the measurements in parallel and crossed polarizer and analyzer, respectively.

The transmitted light can be represented as a sum of a coherent (average) and incoherent (fluctuating) components. Equations for their description are known as the Dyson and the Bethe–Salpeter equations, respectively [29, 36, 38, 39]. We consider only the coherent field. To find it, we use the Foldy–Twersky formalism, which was described in [36] for the scalar field.

For a layer of anisotropic LC droplets, the Foldy–Twersky vector integral equation is written as [24]

$$\begin{pmatrix} E_y \\ E_z \end{pmatrix} = \begin{pmatrix} \psi_y(x)\,|_{x=l} & 0 \\ 0 & \psi_z(x)\,|_{x=l} \end{pmatrix} \begin{pmatrix} \cos\alpha \\ \sin\alpha \end{pmatrix}, \quad (1)$$

where E_y and E_z are the y- and z-components of the coherent field in the case of the unit amplitude of the incident wave, while the functions $\psi_{y,z}(x)$ are solutions of integral equations

$$\psi_{y,z}(x) = \exp(ikx) \times \left(1 - q\left\langle S_{2,1}^0 \right\rangle \int_0^x \exp(-ikx')\psi_{y,z}(x')dx'\right). \quad (2)$$

Here, $q = 2\pi k^{-2} N_v$; $k = 2\pi n_p/\lambda$, where n_p is the refractive index of the anchoring polymer, λ is the wavelength of the incident light; N_v is the number of LC droplets per unit volume; and $\left\langle S_{2,1}^0 \right\rangle$ are the diagonal elements of the amplitude scattering matrix at a zero scattering angle averaged over the droplet size. Hereinafter, the angle brackets $\langle \ldots \rangle$ denote the averaging over the droplet size. In the general case, in which droplets have different internal structures, additional corresponding averaging is necessary.

For the geometrical configuration presented in Fig. 1, the wave that is polarized along the y axis is extraordinary, while the wave polarized along the z axis is ordinary.

The solution of Eq. (2) has the form

$$\psi_{y,z}(x) = \exp(ik_{2,1}x), \quad (3)$$

where k_2 and k_1 are the propagation constants that correspond to the extraordinary and ordinary waves,

$$k_{2,1} = k + iq\left\langle S_{2,1}^0 \right\rangle. \quad (4)$$

In order to determine the amplitude transmission coefficients T_a^{vv} and T_a^{vh} of the PDLC layer for the vv- and vh-polarizations, we will write the following relations:

$$T_a^{vv} = \mathbf{e}_{vv} \underline{\underline{\Psi}} \mathbf{e}_{vv}, \quad (5)$$

$$T_a^{vh} = \mathbf{e}_{vh} \underline{\underline{\Psi}} \mathbf{e}_{vv}, \quad (6)$$

$$\underline{\underline{\Psi}} = \begin{pmatrix} \exp(ik_2 l) & 0 \\ 0 & \exp(ik_1 l) \end{pmatrix}. \quad (7)$$

Performing necessary transformations, we find from (5)–(7) that

$$T_a^{vv} = t_e \cos^2\alpha + t_o \sin^2\alpha, \quad (8)$$

$$T_a^{vh} = (t_o - t_e)\sin\alpha\cos\alpha, \quad (9)$$

where t_e and t_o are the amplitude transmission coefficients of the PDLC layer for the extraordinary (e) and ordinary (o) waves,

$$t_{e,o} = \exp(ikl)\exp(-iq\langle \mathrm{Im} S_{2,1}^0\rangle l)\exp(-q\langle \mathrm{Re} S_{2,1}^0\rangle l). \quad (10)$$

It is convenient to transform expression (10) to the form

$$t_{e,o} = \exp(ikl)\exp(-\phi_{e,o})\exp(-\gamma_{e,o} l/2). \quad (11)$$

Here,

$$\phi_{e,o} = q\left\langle \mathrm{Im}\, S_{2,1}^0 \right\rangle l, \quad (12)$$

$$\gamma_{e,o} = N_v \left\langle \sigma_{e,o} \right\rangle, \quad (13)$$

$$\left\langle \sigma_{e,o} \right\rangle = \frac{4\pi}{k^2}\left\langle \mathrm{Re}\, S_{2,1}^0 \right\rangle, \quad (14)$$

where ϕ_e and ϕ_o are the phase differences for the extraordinary and ordinary waves that were accumulated along thickness l of the PDLC layer; γ_e and γ_o are the extinction indices of the layer for the extraordinary and ordinary waves; and $\langle\sigma_e\rangle$ and $\langle\sigma_o\rangle$ are the corresponding average values of the extinction cross sections for the individual LC droplet, which are determined in accordance with the optical theorem [39].

The coefficient of coherent (direct) transmission of the PDLC layer T_c^p upon its illumination in the absence of an analyzer can be written as follows:

$$T_c^p = T_c^{vv} + T_c^{vh}. \quad (15)$$

Here, T_c^{vv} and T_c^{vh} are the coherent transmission coefficients for the parallel and crossed polarizer and analyzer, respectively,

$$T_c^{vv} = \left|T_a^{vv}\right|^2, \quad (16)$$

$$T_c^{vh} = \left|T_a^{vh}\right|^2. \quad (17)$$

In order to find coherent transmission coefficient T_c^{np} upon illumination by unpolarized light, it is necessary to average T_c^p over polarization angle α. Using expressions (8), (9), and (15)–(17), we obtain

$$T_c^{np} = \frac{T_c^p(\alpha = 0) + T_c^p(\alpha = \pi/2)}{2}. \quad (18)$$

Relations (16)–(18) allow one to analyze the coherent transmission coefficients of the PDLC layer upon its illumination by polarized and unpolarized light in the case of polydisperse oriented droplets of the same internal structure. We can easily find from formulas (8), (9), (11), and (15)–(18) that

$$T_c^p = \exp(-\gamma_e l)\cos^2\alpha + \exp(-\gamma_o l)\sin^2\alpha, \quad (19)$$

$$T_c^{np} = \frac{\exp(-\gamma_e l) + \exp(-\gamma_o l)}{2}. \quad (20)$$

As a rule, the relative refractive index of LC droplets dispersed into a polymer slightly differs from unity [4, 8]. Therefore, we used the anomalous diffraction approximation [22–26, 37]. It allows one to analyze the light scattering by large optically soft LC droplets: the size parameter is $\rho = ka \gg 1$, $|n_{LC} - 1| \ll 1$, where n_{LC} is the maximum relative refractive index of the LC, which, in the general case, can be complex. In terms of this approximation, the scattered field in the far zone is determined as a result of the diffraction by an equivalent plane amplitude–phase screen [39] with a complex transmission matrix that is defined on the principal cross section of the droplet, $\sigma = \pi bc$, where b and c are the semiaxes of the droplet along the y and z axes of the laboratory coordinate system in the plane that is orthogonal to the direction of incidence of the light (x axis). For elements $S_{2,1}^0$ of the amplitude scattering matrix, using relations obtained in [30], we have

$$S_{2,1}^0 = \frac{k^2}{2\pi}\int_\sigma (1 - T_{2,1}(y,z))dydz. \quad (21)$$

Here, $T_{2,1}(y,z)$ are the diagonal elements of the Jones matrix $\underline{\underline{T}}(y,z)$ [40] for the equivalent amplitude–phase screen, which is identified with the LC droplet,

$$\underline{\underline{T}}(y,z) = \prod_{x=x_{inp}(y,z)}^{x=x_{out}(y,z)} R^T(x) P R(x). \quad (22)$$

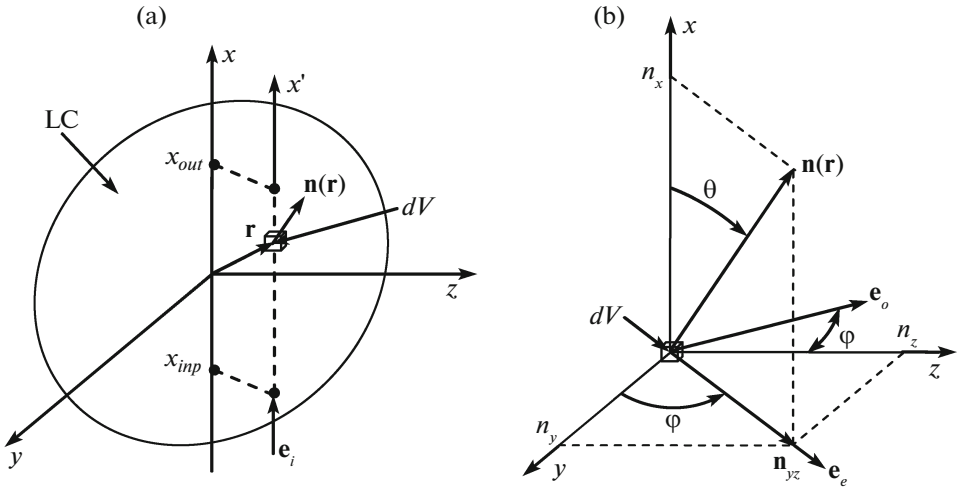

Fig. 2. Schematic representation of the geometry of (a) a droplet with an arbitrary internal structure and (b) its elementary volume dV. Here, **n**(r) is the local director for the elementary volume dV at the point with radius vector **r**; x_{inp} and x_{out} are the coordinates of the input and output of the ray on the surface of the LC droplet; θ and φ are the polar and azimuthal angles of orientation of the local director; and $\mathbf{e}_o$ and $\mathbf{e}_e$ are the polarization unit vectors of the ordinary and extraordinary waves at point **r**.

In expression (22), x_{inp} and x_{out} are the coordinates of the input and output of the ray on the surface of the LC droplet, which depend on y and z (Fig. 2a); P is the matrix of local accumulated phase differences for the extraordinary and ordinary waves; $R(x)$ is the matrix of transformation (rotation) of the local basis to the laboratory one; and $R^T(x)$ is the transposed matrix of the inverse transformation. The latter three matrices are expressed as follows:

$$P = \begin{pmatrix} \exp(ik(n_e(x)/n_p - 1)\Delta x) & 0 \\ 0 & \exp(ik(n_o/n_p - 1)\Delta x) \end{pmatrix}, \quad (23)$$

$$R(x) = \begin{pmatrix} \cos\varphi(x) & -\sin\varphi(x) \\ \sin\varphi(x) & \cos\varphi(x) \end{pmatrix}, \quad (24)$$

and

$$R^T(x) = \begin{pmatrix} \cos\varphi(x) & \sin\varphi(x) \\ -\sin\varphi(x) & \cos\varphi(x) \end{pmatrix}. \quad (25)$$

Here, $n_e(x)$ is the local refractive index for the extraordinary wave at point $x = x(y, z)$; n_o is the refractive index for the ordinary wave, which does not depend on the coordinates x, y, and z and is equal to ordinary refractive index $n_\perp$ of the LC; Δx is the longitudinal size of elementary volume dV along the direction of propagation of the light; and $\varphi(x)$ is the azimuthal angle of orientation of the local principal plane at the point $x = x(y, z)$ (Fig. 2b).

In Fig. 2, **n**(**r**) is the local director of elementary volume dV at the point with radius vector **r**, $|\mathbf{n}(\mathbf{r})| = 1$; θ is the polar angle of orientation of the local director; n_x, n_y, and n_z are the Cartesian components of the local director **n**(**r**); and $\mathbf{e}_o$ and $\mathbf{e}_e$ are the unit polarization vectors of the ordinary and extraordinary waves at point **r**.

It can be seen from Fig. 2b that the local refractive index $n_e(x)$ for the extraordinary wave and the values of the cosine and sine of the azimuth $\varphi(x)$ of orientation of the local principal plane are expressed via the components n_x, n_y, and n_z of the local director as follows:

$$\begin{aligned} n_e &= n_\parallel n_\perp / \sqrt{n_\parallel^2 \cos^2\theta + n_\perp^2 \sin^2\theta} \\ &= n_\parallel n_\perp / \sqrt{n_\parallel^2 n_x^2 + n_\perp^2 (1 - n_x^2)}, \end{aligned} \quad (26)$$

where $n_\parallel$ is the extraordinary refractive index of the LC,

$$\cos\varphi(x) = n_y / \sqrt{1 - n_x^2}, \quad (27)$$

$$\sin\varphi(x) = n_z / \sqrt{1 - n_x^2}. \quad (28)$$

Analysis of expressions (21)–(28) shows that, if the anisometry of LC droplets in the layer is the same, i.e., the semiaxes a, b, and c of the droplet obey the relations $\varepsilon_y = b/a = \text{const}$ and $\varepsilon_z = c/a = \text{const}$, then, at the same configuration of the director in the droplet volume, the elements $S_{2,1}^o$ of the amplitude scattering matrix at zero scattering angle depend only on the longitudinal axis a,

$$S_{2,1}^o = S_{2,1}^o(a). \quad (29)$$

As can be seen from formulas (13), (14), and (29), in order to calculate γ_e and γ_o, it is necessary to know the distribution function $P(a)$ of the longitudinal semiaxis. Finding it is a complicated problem, because it is necessary to experimentally analyze a large number of transverse sections of the specimen. Therefore,

we will consider another method of finding γ_e and γ_o that makes it possible to determine values of the longitudinal semiaxis from measurements of the transmission coefficient of the layer.

Using expressions (13) and (14) and taking into account formula (29), we have

$$\gamma_{e,o} = N_v \frac{4\pi}{k^2} \int_{a_1}^{a_2} \mathrm{Re}\, S_{2,1}^0(a) P(a) da, \tag{30}$$

where a_1 and a_2 are the minimum and maximum values of the longitudinal semiaxis a for the ensemble of LC droplets in the layer. Based on the mean-value theorem, this formula can be written as follows:

$$\begin{aligned}\gamma_{e,o} &= N_v \frac{4\pi}{k^2} \mathrm{Re}\, S_{2,1}^0(a_{\mathrm{ef}}^{e,o}) \int_{a_1}^{a_2} P(a) da \\ &= N_v \frac{4\pi}{k^2} \mathrm{Re}\, S_{2,1}^0(a_{\mathrm{ef}}^{e,o}).\end{aligned} \tag{31}$$

Here, a_{ef}^e and a_{ef}^o are the effective values of the longitudinal semiaxis upon consideration of the extinction of the extraordinary and ordinary waves, respectively, $a_1 \le a_{\mathrm{ef}}^{e,o} \le a_2$. The distribution function $P(a)$ is normalized as follows:

$$\int_{a_1}^{a_2} P(a) da = 1. \tag{32}$$

As a result, expressions (19) and (20) can be written as

$$T_c^p = \exp(-\gamma_e(a_{\mathrm{ef}}^e) l)\cos^2\alpha + \exp(-\gamma_o(a_{\mathrm{ef}}^o) l)\sin^2\alpha, \tag{33}$$

$$T_c^{np} = \frac{\exp(-\gamma_e(a_{\mathrm{ef}}^e) l) + \exp(-\gamma_o(a_{\mathrm{ef}}^o) l)}{2}. \tag{34}$$

As is seen from expression (33), the effective values a_{ef}^e and a_{ef}^o of the longitudinal semiaxis a can be found from comparison of numerical calculations with experimental data for the coherent transmission coefficient T_c^p upon illumination of the PDLC layer by light the polarization angle of which is $\alpha = 0$ and $\alpha = \pi/2$, respectively. The values of a_{ef}^e and a_{ef}^o can also be found if the distribution function $P(a)$ of longitudinal semiaxes is known a priori. Below, in a separate section, we compare the data on the coherent transmission coefficient calculated in terms of the described model with experiment.

We emphasize that the obtained relationships make it possible to analyze the coherent transmission coefficient of the PDLC layer based on the data on the configuration of the director $\mathbf{n}(\mathbf{r})$ in the volume of the LC droplet. This configuration depends on the boundary conditions on the droplet surface and on the controlling field. At specified boundary conditions, the configuration of the director $\mathbf{n}(\mathbf{r})$ in the volume of the LC droplet is found from the solution of the problem of minimization of the free energy volume density [1].

THE CALCULATION TECHNIQUE OF INTERNAL ORIENTATIONAL STRUCTURES OF NEMATIC LC DROPLETS

The internal orientational structure of LC droplets in a polymer matrix is determined by the following main factors [8, 41, 42]: (i) the intermolecular interaction in the LC, which leads to the ordering of molecules that is characteristic of a given LC phase (nematic, cholesteric, smectic, etc.); (ii) the interaction with the polymer, which, depending on the interphase boundary conditions on the surface of the droplet, causes LC molecules to be oriented either along its boundary (tangential boundary conditions) or perpendicularly to it (normal boundary conditions); (iii) and the external electric (or magnetic) field. Molecules in the LC droplet are oriented so as to ensure a minimum in the free energy.

In the single-constant approximation [1], the following differential equation can be written for the vector field of the local director $\mathbf{n}(\mathbf{r})$ corresponding to the minimum of the free energy density:

$$K\Delta\mathbf{n}(\mathbf{r}) + \varepsilon(\mathbf{E}, \mathbf{n}(\mathbf{r}))\mathbf{E} = 0. \tag{35}$$

Here, Δ is the Laplace operator; K is the elastic constant of the LC; $\varepsilon = \varepsilon_0\Delta\varepsilon$, where $\varepsilon_0 = 8.85 \times 10^{-12}\mathrm{C}^2/(\mathrm{N\ m}^2)$ is the electric constant and $\Delta\varepsilon$ is the dielectric anisotropy of the LC; and $\mathbf{E}$ is the external controlling electric field vector.

Upon solving Eq. (35) in a Cartesian coordinate system, in order to find the components n_x, n_y, and n_z of local director $\mathbf{n}(\mathbf{r})$, we use the difference scheme of calculations [43]. For point $\mathbf{r} = (0, 0, 0)$ in the center of the LC droplet, we have

$$\begin{aligned}&K\left(\frac{n_x(-1,0,0) + n_x(1,0,0) - 2n_x}{(\Delta x)^2}\right. \\ &\quad + \frac{n_x(0,-1,0) + n_x(0,10) - 2n_x}{(\Delta y)^2} \\ &\quad \left. + \frac{n_x(0,0,-1) + n_x(0,0,1) - 2n_x}{(\Delta z)^2}\right) \\ &+ \varepsilon E_x(E_x n_x + E_y n_y + E_z n_z) = 0,\end{aligned} \tag{36}$$

$$\begin{aligned}&K\left(\frac{n_y(-1,0,0) + n_y(1,0,0) - 2n_y}{(\Delta x)^2}\right. \\ &\quad + \frac{n_y(0,-1,0) + n_y(0,10) - 2n_y}{(\Delta y)^2} \\ &\quad \left. + \frac{n_y(0,0,-1) + n_y(0,0,1) - 2n_y}{(\Delta z)^2}\right) \\ &+ \varepsilon E_y(E_x n_x + E_y n_y + E_z n_z) = 0,\end{aligned} \tag{37}$$

$$K\left(\frac{n_z(-1,0,0)+n_z(1,0,0)-2n_z}{(\Delta x)^2}+\frac{n_z(0,-1,0)+n_z(0,10)-2n_z}{(\Delta y)^2}+\frac{n_z(0,0,-1)+n_z(0,0,1)-2n_z}{(\Delta z)^2}\right)+\varepsilon E_z(E_x n_x+E_y n_y+E_z n_z)=0, \quad (38)$$

$$n_x^2+n_y^2+n_z^2=1, \quad (39)$$

where Δx, Δy, and Δz are the iteration steps along the corresponding axes of the laboratory coordinate system (x, y, z) upon discretization of expression (35); E_x, E_y, and E_z are the values of the projections of electric field vector **E** onto the corresponding coordinate axes.

The calculation technique of the internal orientational structure of the LC droplet is as follows. (i) Initially, some certain orientation of the director in the volume of the droplet is specified; (ii) the volume of the droplet is then divided into cells and the orientation of local director $\mathbf{n} = \mathbf{n}(\mathbf{r})$ in each cell is sought; and (iii) after that, the components n_x, n_y, and n_z of the local director in the cell with the coordinates x, y, and z are found from Eqs. (36)–(38). At each subsequent iteration, the influence of the strictly specified orientation of the director at the interface is extended further into the volume of the droplet. As a result, this iterative procedure (relaxation method) leads to the determination of the orientational structure of the nematic LC droplet that corresponds to a minimum of the free energy of its entire volume. In this case, we can assume at a first approximation that the surface of the LC droplet is divided into two characteristic areas (Fig. 3), in which the long axes of molecules of the LC droplet are directed along the normal to the surface (normal boundary conditions) and along the tangent to it (tangential boundary conditions). Figure 3 shows a schematic representation of the LC droplet in the shape of an ellipsoid. In order to quantitatively determine the degree of inhomogeneity of the interphase surface anchoring of the LC with the polymer matrix, we will use the parameter w (Fig. 3). It characterizes the area of the droplet with normal surface anchoring. We note that the values $w = 0\%$ and $w = 100\%$ correspond to homogeneous surface anchoring on the LC–polymer surface. At $w = 0\%$, only tangential surface anchoring occurs and a bipolar configuration of the LC is formed in the droplet. At $w = 100\%$, only normal surface anchoring is realized and the internal structure of the droplet is radial.

The parameter w depends on the external controlling field, which leads to an electrically controllable change of the internal structure of droplets and, correspondingly, their optical characteristics and characteristics of the layer as a whole. In practice, as was already noted above, a change in the parameter w in the field is realized by using surface-active substances, surfactants [16, 17].

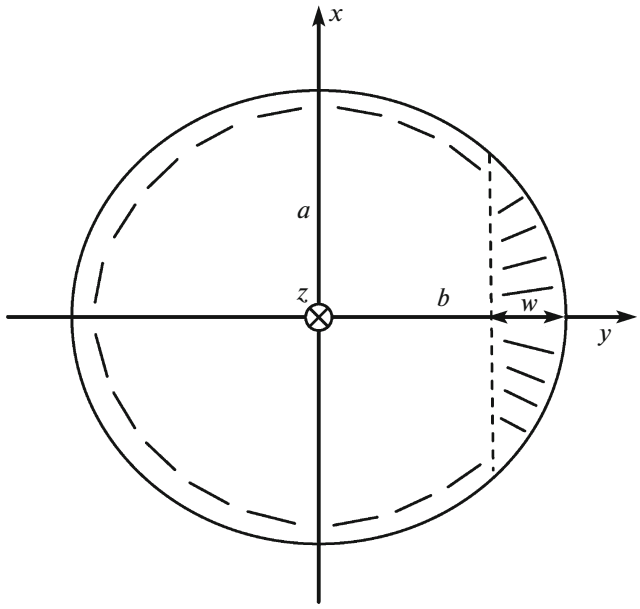

Fig. 3. Schematic representation of the cross-section of a LC droplet with inhomogeneous boundary conditions in the (x, y) plane. The parameter w characterizes the fraction of the surface of the droplet with normal (homeotropic) surface anchoring, and a and b are the semiaxes of the droplet.

ANALYSIS OF RESULTS AND COMPARISON WITH EXPERIMENT

Let us compare results that were obtained in framework of the developed optical model with experimental data. We will use the experimental dependence of the electrooptical response (the dependence of the coherent transmission coefficient T_c^p on strength of the applied field E) that was presented in [44] for a PDLC layer upon the field transition corresponding to the initial (in the absence of a field) radial configuration of LC droplets (parameter $w = 100\%$) in the layer. Upon application of an external controlling electric field in the plane of the specimen, the parameter w decreases.

A composite film was prepared based on the 5CB LC, with its ordinary refractive index at wavelength $\lambda = 0.658$ μm being $n_\perp = 1.531$ and the extraordinary one being $n_\parallel = 1.717$. As a polymer matrix, polyvinyl alcohol (PVA) plasticized with glycerol was chosen. The LC was doped with the CTAB surfactant. The PVA : glycerol : 5CB : CTAB weight proportion was 9.3 : 3.7 : 1 : 0.02, which, in terms of volume concentration c_v of LC droplets, yielded $c_v = (1 + 0.02)/(9.3 + 3.7) \approx 0.078$. The thickness of the film was $l = 16$ μm. The concentration of LC droplets in the

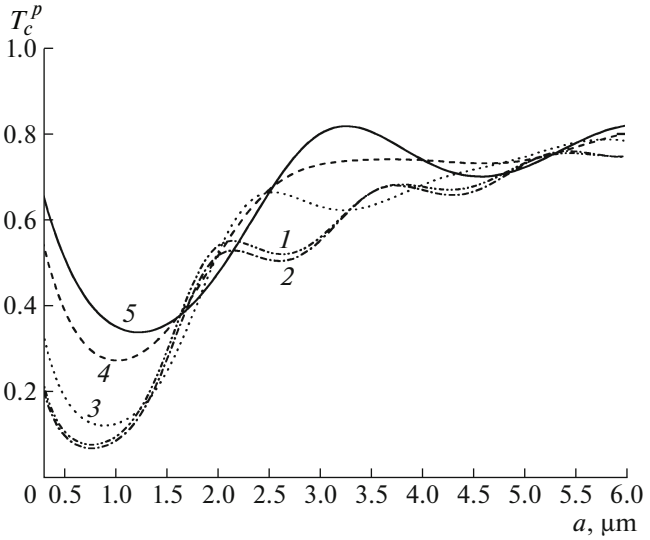

Fig. 4. Values of the coherent transmission coefficient T_c^p of a PDLC film calculated in relation to radius a of spherical droplets of the 5CB LC ($n_\perp = 1.531$, $n_\parallel = 1.717$). $w =$ (curve *1*) 0, (*2*) 25, (*3*) 50, (*4*) 75, and (*5*) 100%. $\alpha = 0$, $n_p = 1.515$, $\lambda = 0.658$ μm, $c_v = 0.073$, and $l = 16$ μm.

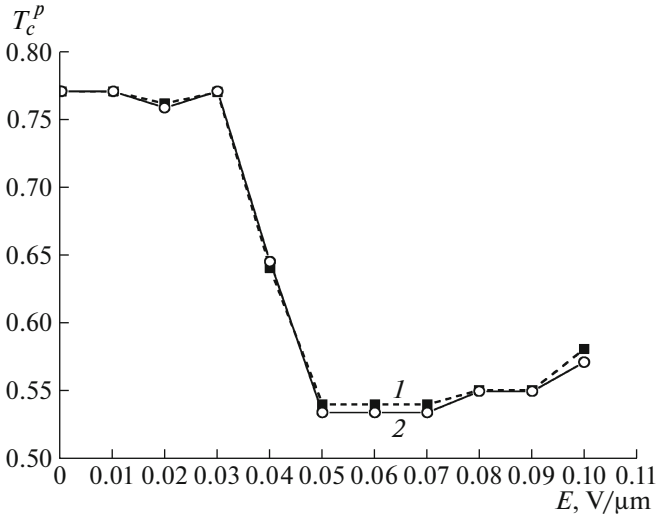

Fig. 5. (*1*) Experimental and (*2*) calculated dependences of the transmission coefficient T_c^p on the controlling field strength for a composite PDLC film with inhomogeneous interphase surface anchoring. The polarization vector of the incident wave is parallel to the y axis. The 5CB LC was used ($n_\perp = 1.531$, $n_\parallel = 1.717$). $\alpha = 0$, $n_p = 1.515$, $\lambda = 0.658$ μm, $c_v = 0.073$, $l = 16$ μm, and $a_{ef}^e = 2.85$ μm.

prepared specimen decreased because of dissolving of the LC in the polymer and due to the occurrence of residual water. In numerical calculations, the volume concentration of LC droplets in the PDLC layer was taken to be $c_v = 0.073$. With a chosen amount of the surfactant (2 wt % with respect to LC), the normal surface anchoring and the radial configuration of LC droplets in the absence of a controlling field ($w =$ 100%) were realized. Under the action of the field, the inverse regime of the ionic modification of interphase boundaries was realized, in which the fraction of the tangential anchoring to the polymer increased [17]. The refractive index of the used polymer was $n_p =$ 1.532. Addition of glycerol reduced the refractive index of the specimen to the value of $n_p = 1.515$. The specimen was illuminated along its normal. The polarization vector of the incident wave was parallel to the y axis ($\alpha = 0$). The vector of applied electric field was directed along the y axis. The transverse size of droplets in the plane of the film was in the range of 2–3 μm. Polarization-microscopy measurements showed that, in the absence of mechanical tension of the PDLC film, droplets had a spherical shape, with the anisometry parameters being $\varepsilon_y = \varepsilon_z = 1$. The value of the coherent transmission coefficient in the absence of a field was $T_c^p = 0.77$ (in this case, the photon mean free path was ~60 μm).

Figure 4 presents the dependences of the transmission coefficient T_c^p on radius a of LC droplets in the layer calculated at different values of the parameter w.

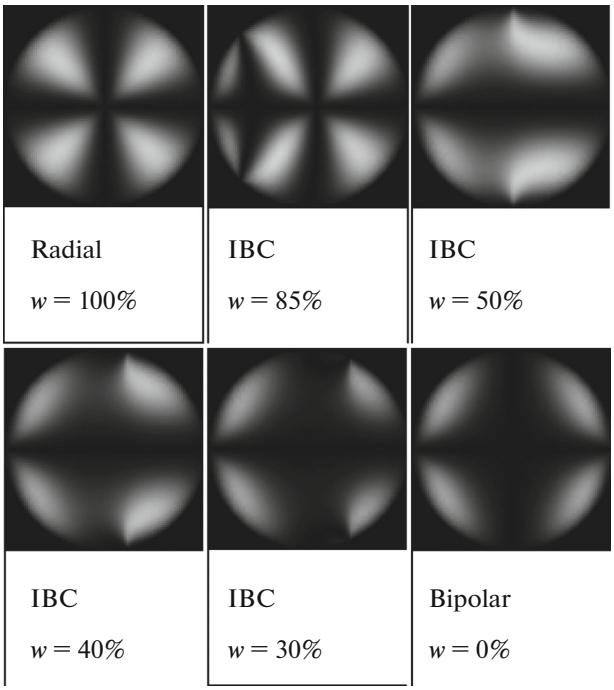

Fig. 6. Calculated textures of LC droplets in crossed polarizers. The first texture corresponds to the normal surface anchoring ($w = 100\%$), while the last one corresponds to the tangential surface anchoring ($w = 0\%$). The remaining textures were obtained at inhomogeneous surface anchoring (inhomogeneous boundary conditions (IBC)) at the values $w = 85$, 50, 40, and 30%, which were used in the experiment (Fig. 5 and table).

Calculated and experimental data for the coherent transmission coefficient T_c^p of a PDLC film with inhomogeneous interphase boundaries and retrieved values of the parameter w at different strengths of the controlling field

E, V/μm	T_c^p, experiment	ΔT	w, %	T_c^p, theory
0.0	0.77	0.0	100.0	0.7699
0.01	0.77	0.0	100.0	0.7699
0.02	0.761	0.009	85.0	0.7578
0.03	0.77	0.0	100.0	0.7699
0.04	0.64	0.13	50.0	0.6447
0.05	0.54	0.23	30.0	0.5337
0.06	0.54	0.23	30.0	0.5337
0.07	0.54	0.23	30.0	0.5337
0.08	0.55	0.22	35.0	0.5494
0.09	0.55	0.22	35.0	0.5494
0.1	0.58	0.19	40.0	0.5708

The first column contains values of strength of the field E. The second column lists experimental values of the transmission coefficient T_c^p. The third column represents differences of experimental values of the transmission coefficient determined at $E = 0$ and at a specified value of E: $\Delta T = T_c^p(E = 0) - T_c^p(E \neq 0)$. The fourth column yields retrieved values of the parameter w. The fifth column yields calculated values of the transmission coefficient T_c^p.

The shape of each of them is determined by the oscillating character of the dependence of the extinction efficiency factor of the LC droplet. As can be seen from the comparison of these results with the experimental data of Fig. 5, the radius $a = 2.85$ μm corresponds to the experimental value of the transmission coefficient $T_c^p = 0.77$ at $w = 100\%$, which is realized in the absence of a field ($E = 0$) (Fig. 4). It determines the value of effective size a_{ef}^e of the droplet in expression (33). Therefore, $a_{\text{ef}}^e = 2.85$ μm.

The further procedure of comparison with experiment was the calculation of the transmission coefficient $T_c^p(\alpha = 0)$ at the fixed value $a_{\text{ef}}^e = 2.85$ μm and varied parameter w and of the determination (retrieval) of values of w that correspond to the experimentally measured values of the transmission of the specimen in the applied electric field E. Results of this comparison are presented in Fig. 5 and in the table. The table also shows experimental values of the modulation depth in the forward-transmitted light $\Delta T = T_c^p(E = 0) - T_c^p(E \neq 0)$, where E is the controlling field strength. The discrepancy between the theoretical and experimental data on the transmission upon retrieval of w did not exceed 1.6%.

Figure 6 shows textures of the LC droplet for the retrieved values of the transmission coefficient of the layer. The first texture, which has the shape of a Maltese cross, corresponds to completely homogeneous normal boundary conditions and radial configuration of the LC droplet. The four subsequent textures were constructed at values of w that correspond to the values of the applied voltage at which measurements of the transmission were performed (see table). The last of the presented textures is realized at tangential surface anchoring.

From the data presented in Figs. 5 and 6 and in the table, we can conclude that the structure of LC droplets in the controlling field does not change from the radial structure (for which $w = 100\%$) to the bipolar one (for which $w = 0\%$). As follows from the comparison of the theoretical and experimental data, the minimal value of w is 30%. This is likely to be determined by the energetically favorable balance between the elastic and dielectric components of the volume energy at the used concentration of the surfactant in the specimen under investigation in the considered range of variation of the controlling field.

As follows from Fig. 4, for the considered modification of interphase boundaries, the modulation of the coherent transmission coefficient is caused by a decrease in the fraction of the droplet surface with normal surface anchoring and by an increase in the fraction of the surface with tangential surface anchoring.

CONCLUSIONS

We developed an optical model for the description of the coherent transmission coefficient of a layer of anisotropic droplets in an isotropic matrix. It is based on the extension of the Foldy–Twersky and the anomalous diffraction approximations to the vector case for a layer of LC droplets with an arbitrary internal structure.

The model allows one to analyze the coherent transmission coefficients of a PDLC layer upon its normal illumination of linearly polarized and unpolarized radiation in relation to the size of LC droplets, their anisometry, the concentration, the layer thickness, the refractive index of the LC, and the internal structure of droplets. In order to find the internal structure of LC droplets, we used the relaxation method of solving the problem of minimization of the free energy volume density in the single-constant approximation. We compared theoretical and experimental data for a PDLC layer of polydisperse ellipsoidal droplets of a nematic LC with inhomogeneous interphase surface anchoring. The developed optical model makes it possible to solve problems of optimization of the electrooptical response of such films. We proposed a technique for determination of the size of LC droplets using data on the dependence of the transmission coefficient on the applied voltage.

ACKNOWLEDGMENTS

This work was supported by the National Academy of Sciences of Belarus and the Siberian Branch of the Russian Academy of Sciences (project no. 36) and the Belarusian Republican Foundation for Fundamental Research (project no. F15SO-039).

REFERENCES

1. L. M. Blinov and V. G. Chigriniv, *Electrooptic Effects in Liquid Crystal Materials* (Springer, New York, 1993).
2. *Flexible Flat Panel Displays,* Ed. by G. P. Crawford (Wiley, Hoboken, 2005).
3. J. A. Castellano, *Liquid Gold: The Story of Liquid Crystal Displays and the Creation of an Industry* (World Scientific, Singapore, 2005).
4. F. Simoni, *Nonlinear Properties of Liquid Crystals and Polymer Dispersed Liquid Crystals* (World Scientific, Singapore, 1997).
5. *Display Systems,* Ed. by L. W. MacDonald and A. C. Lowe (Wiley, New York, 1997).
6. V. G. Chigrinov, *Liquid Crystal Devices: Physics and Application* (Artech House, Boston, London, 1999).
7. G. E. Volovik and O. D. Lavrentovich, Sov. Phys. JETP **58**, 1159 (1983).
8. P. S. Drzaic, *Liquid Crystal Dispersions* (World Scientific, Singapore, 1995).
9. J. L. West, J. W. Doane, and S. Zumer, US Patent No. 4685771 (1987).
10. V. K. Freedericksz and V. Zolina, Trans. Faraday Soc. **29**, 919 (1933).
11. E. Dubois-Violette and P. G. de Gennes, J. Phys. Lett. **36**, L255 (1975).
12. L. M. Blinov, E. I. Kats, and A. A. Sovin, Sov. Phys. Usp. **30**, 604 (1987).
13. G. Ryschenkow and M. Kléman, J. Chem. Phys. **64**, 404 (1976).
14. L. M. Blinov, N. N. Davydova, A. A. Sonin, et al., Sov. Phys. Crystallogr. **29**, 320 (1984).
15. L. Komitov, B. Helgee, and J. Felix, Appl. Phys. Lett. **86**, 023502 (2005).
16. V. Ya. Zyryanov, M. N. Krakhalev, O. O. Prishchepa, and A. V. Shabanov, JETP Lett. **86**, 383 (2007).
17. V. Ya. Zyryanov, M. N. Krakhalev, and O. O. Prishchepa, JETP Lett. **88**, 597 (2008).
18. A. Walther and A. Muller, Soft Matter **4**, 663 (2008).
19. A. Perro, S. Reculusa, S. Ravaine, E. Bourgeat-Lami, and E. Duguet, J. Mater. Chem. **15**, 3745 (2005).
20. F. Basile, F. Bloisi, L. Vicari, and F. Simoni, Phys. Rev. E **48**, 432 (1993).
21. V. V. Presnyakov and T. V. Galstian, Mol. Cryst. Liq. Cryst. **413**, 435 (2004).
22. V. A. Loiko and A. V. Konkolovich, J. Exp. Theor. Phys. **103**, 935 (2006).
23. V. A. Loiko and V. I. Molochko, Tech. Phys. **44**, 1340 (1999).
24. J. D. Klett and R. A. Sutheland, Appl. Opt. **31**, 373 (1997).
25. S. Zumer, Phys. Rev. A **37**, 4006 (1988).
26. D. A. Yakovlev and O. A. Afonin, Opt. Spectrosc. **82**, 78 (1997).
27. V. A. Loiko, P. G. Maksimenko, and A. V. Konkolovich, Opt. Spectrosc. **105**, 791 (2008).
28. A. D. Kiselev, O. V. Yaroshchuk, and L. Dolgov, J. Phys.: Condens. Matter **16**, 183 (2004).
29. A. P. Ivanov, A. V. Loiko, and V. P. Dik, *Light Propagation in Densely-Packed Dispersed Media* (Nauka Tekhnika, Minsk, 1988) [in Russian].
30. V. A. Loiko, U. Maschke, V. Ya. Zyryanov, A. V. Konkolovich, and A. A. Miskevich, Opt. Spectrosc. **110**, 110 (2011).
31. A. Khan, I. Shiyanovskaya, T. Schneider, et al., J. SID **15**, 9 (2007).
32. M. N. Krakhalev, V. A. Loiko, and V. Ya. Zyryanov, Tech. Phys. Lett. **37**, 34 (2011).
33. O. O. Prishchepa, A. V. Shabanov, V. Ya. Zyryanov, A. M. Parshin, and V. G. Nazarov, JETP Lett. **84**, 607 (2006).
34. A. Mertelj and M. Čopič, Phys. Rev. E **75**, 011705 (2007).
35. O. O. Prishchepa, M. Kh. Egamov, V. P. Gerasimov, et al., Izv. Vyssh. Uchebn. Zaved., Fiz. **56** (2/2), 258 (2013).
36. A. Ishimaru, *Propagation and Scattering of Waves in Random Media* (Academic, New York, 1978; Mir, Moscow, 1981).
37. H. C. van de Hulst, *Light Scattering by Small Particles* (Dover, New York, 1981; Inostr. Liter., Moscow, 1961).
38. L. G. Apresyan and Yu. A. Kravtsov, *Radiation Transfer* (Gordon Breach, Basel, Switzerland, 1996; Nauka, Moscow, 1983).
39. S. M. Rytov, Yu. A. Kravtsov, and V. I. Tatarskii, *Introduction to Statistical Radiophysics. Random Fields* (Nauka, Moscow, 1978) [in Russian].
40. E. F. Ishchenko and A. L. Sokolov, *Polarizing Optics* (Mosk. Energet. Inst., Moscow, 2005) [in Russian].
41. A. Yu. Val'kov, E. V. Aksenova, and V. P. Romanov, Phys. Rev. E **87**, 022508 (2013).
42. O. O. Prishchepa and A. V. Shabanov, JETP Lett. **84**, 723 (2006).
43. Yu. G. Soloveichik, M. E. Royak, and M. G. Persova, *Finite Element Method for Solving Scalar and Vector Problems* (Novosib. Gos. Tekh. Univ., Novosibirsk, 2007) [in Russian].
44. M. N. Krakhalev, V. A. Loiko, and V. Ya. Zyryanov, Tech. Phys. Lett. **37**, 34 (2011).